

**12022**  
**Ilmenite Basalt**  
**1864.3 grams**



*Figure 1: PET photo of 12022,0 with caked on dirt (before dusting). NASA photo # S69-64108.*

## **Introduction**

Neal et al. (1994) classify 12022 as an ilmenite basalt while James and Wright (1972) had termed it an ilmenite-bearing olivine basalt. It has been dated at 3.2 b.y. All surfaces, except perhaps the flat end, were apparently covered with micrometeorite craters (Hörz et al. 1971), making this rock less than ideal for cosmic-ray depth profiles.

## **Petrography**

The petrography of 12022 is discussed in Weill et al. (1971), Brett et al. (1971), McGee et al. (1977). McGee et al. describe 12022 as “a medium grained porphyritic basalt characterized by subhedral olivine (0.3 mm) and pyroxene (1-2 mm) phenocrysts. Several olivine

phenocrysts are epitaxially overgrown with pyroxene. The matrix consists of feathery intergrowths of parallel feldspar tablets (0.05-1 mm), surrounded ilmenite laths (0.03-0.2 mm), anhedral pyroxene crystals (0.6-0.8 mm) and minor glassy mesostasis”.

Ilmenite in 12022 has an interesting cross-cutting, parallel, skeletal habit.

## **Mineralogy**

**Olivine:** Butler (1972) determined the minor element content of olivine in 12022.



*Figure 2: Reflected light photo of thin section 12022, 10 showing alignment of ilmenite, clumps of pyroxene phenocrysts in fine-grained variolitic groundmass. Field of view 1 cm. NASA photo # S70-24742.*

**Pyroxene:** Weill et al. (1971) and Brett et al. (1971) determined that the cores of pyroxene phenocrysts in 12022 are Ca-rich, zoning outward to Fe-rich (figure 4). The zonation of minor elements (Al, Ti, Cr ) in pyroxene in 12022 is discussed in Bence and Papike (1972).

**Plagioclase:** Plagioclase is An<sub>91-85</sub>.

### Mineralogical Mode of 12022

	McGee et al. 1977	Neal et al. 1994	Brett et al. 1971
Olivine	16-33	19.5	16.5
Pyroxene	30-59	56	58.6
Plagioclase	12-26	12.2	12
Opacites	9-23	~9	11.2
“silica”		0.2	
mesostasis	1	2.3	1.6

**Opacites:** Ilmenite laths occur in groups, cutting trough the matrix but not intersecting the phenocrysts (McGee et al. 1977). Subrounded octahedra of Cr-spinel, with or without rims of Ti-spinel, occur in the matrix and as inclusions in olivine and pyroxene phenocrysts.

**Metal:** Brett et al. (1971) determined the Ni content of minute metallic iron grains in 12022 (figure 5).

### Chemistry

Kushiro et al. (1971), Engel et al. (1971) and Snyder et al. (1997) determined relatively high TiO<sub>2</sub> for 12022 (figure 7). Numerous investigators determined trace elements (table 1, figure 6). Kaplan and Petrowski (1971) determined about 20 ppm carbon and 800 ppm

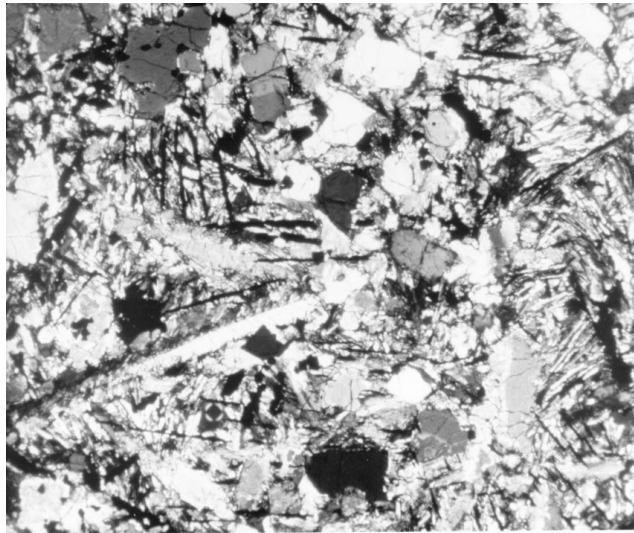
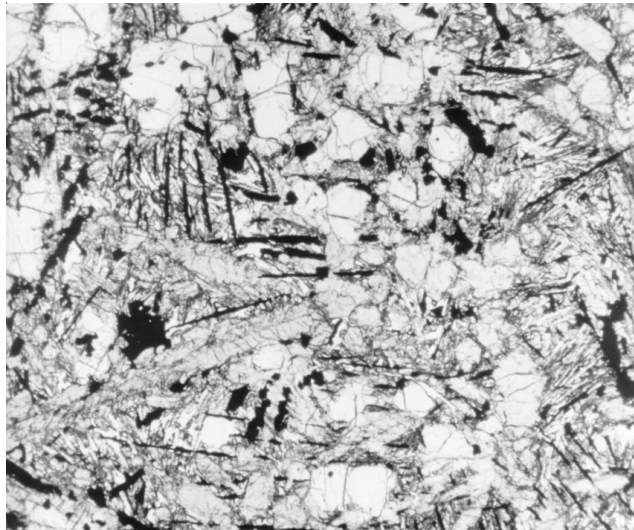


*Figure 3: Photomicrographs of thin section 12022, 9 (plane-polarized, crossed-nicol). Field of view 2.6 mm. NASA phot #s S70-49455-456*

sulfur in 12022. Moore et al. (1971) reported about 40 ppm carbon and 44 ppm nitrogen. Rees and Thode (1972) reported 914 ppm sulfur.

### Radiogenic age dating

Alexander et al. (1972) determined an age for 12022 of  $3.18 \pm 0.04$  b.y. by the Argon plateau method. Snyder et al. (1997) reported the isotopic composition of Sr and Nd.

### Cosmogenic isotopes and exposure ages

Not reported !

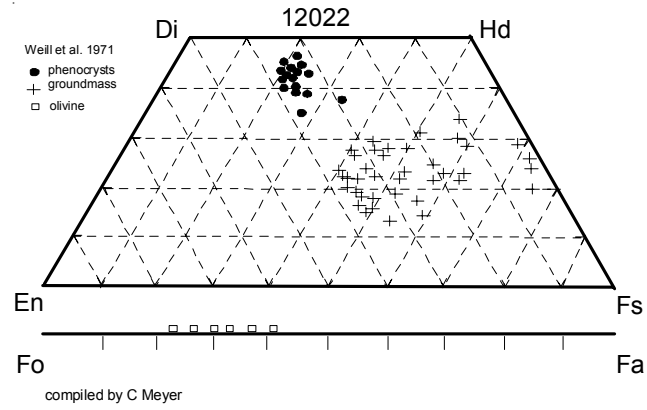


*Figure 4: Pyroxene and olivine composition for 12022 (adapted from Weill et al. 1971, Brett et al. 1971).*

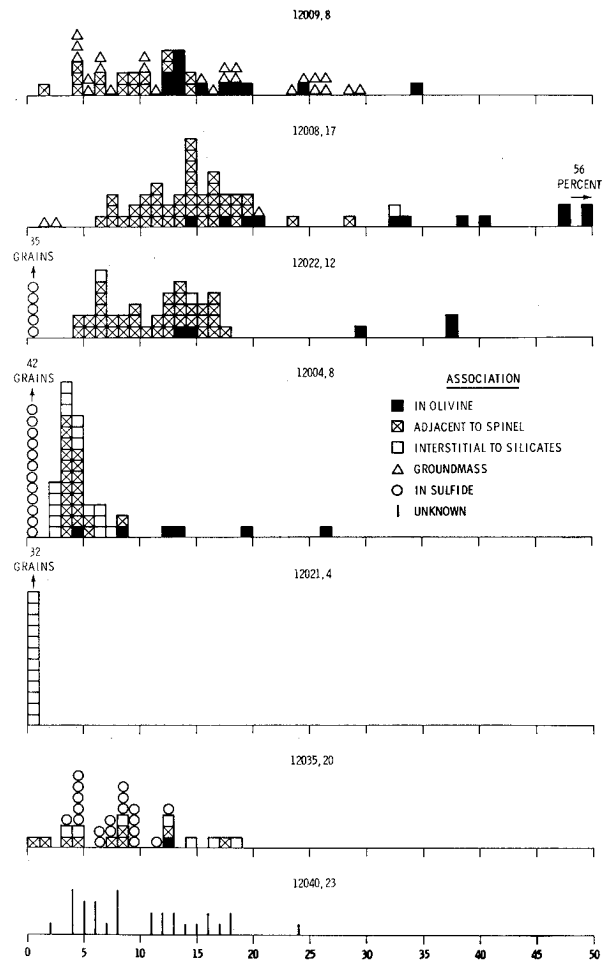


*Figure 5: Histogram of Ni concentrations of metal grains in 7 lunar samples (lifted from Brett et al. 1971).*

**Table 1a. Chemical composition of 12022.**

reference	Kushiro71	LSPET70	Hubbard71	Weismann75	Murthy71	Haskin71	Engel71	Taylor71	Tats71
weight	1 g		188 mg	188 mg					
SiO <sub>2</sub> %	42.33	(a) 36					43.2	(a)	
TiO <sub>2</sub>	4.54	(a) 5.1					5.16	(a)	
Al <sub>2</sub> O <sub>3</sub>	9.12	(a) 11					9.04	(a)	
FeO	22.06	(a) 22					21.44	(a)	
MnO	0.26	(a) 0.17					0.25	(a)	
MgO	11.58	(a) 13					10.43	(a)	
CaO	9.37	(a) 11					9.56	(a)	
Na <sub>2</sub> O	0.29	(a) 0.36	0.24				0.47	(a)	
K <sub>2</sub> O	0.07	(a) 0.068	0.065	(b) 0.065	(b) 0.051	(b)	0.07	(a)	
P <sub>2</sub> O <sub>5</sub>	0.02	(a)					0.13	(a)	
S %									
sum									
Sc ppm		52					55	55	(d)
V		65					180	150	(d)
Cr	3831	(a) 2650					3800	3300	(d)
Co		36					44	52	(d)
Ni		40					42	42	(d)
Cu							8	5	(d)
Zn									
Ga									
Ge ppb									
As									
Se									
Rb	0.17		0.738	(b) 0.738	(b) 0.819	(b)			
Sr	160		143	(b) 143	(b) 138	(b)	130	140	(d)
Y	62						68	64	(d)
Zr	160						180	135	(d)
Nb								6	(d)
Mo									
Ru									
Rh									
Pd ppb									
Ag ppb									
Cd ppb									
In ppb									
Sn ppb								0.39	(d)
Sb ppb									
Te ppb									
Cs ppm									
Ba	38		59.5	(b) 148	(b)		70	60	(d)
La						5.81	(c )	6.3	(d)
Ce	17.4	(b) 17.4		(b)		16.7	(c )	19	(d)
Pr								3	(d)
Nd	14.4	(b) 14.4		(b)		19	(c )	16	(d)
Sm	5.38	(b) 5.38		(b)		6.31	(c )	6.4	(d)
Eu	1.26	(b) 1.26		(b)		1.32	(c )	1.4	(d)
Gd	7.71	(b) 7.71		(b)		9.2	(c )	9.7	(d)
Tb						1.56	(c )	1.8	(d)
Dy	9.37	(b) 9.37		(b)		10.8	(c )	12	(d)
Ho						1.87	(c )	3	(d)
Er	5.42	(b) 5.42		(b)		5.8	(c )	8.2	(d)
Tm								1.3	(d)
Yb	5.69	(b) 5.06		(b)		5.34	(c ) 10	7.2	(d)
Lu						0.767	(c )		
Hf			0.18	(b)				5.2	(d)
Ta									
W ppb									
Re ppb									
Os ppb									
Ir ppb									
Pt ppb									
Au ppb									
Th ppm							0.75	(d) 0.71	(b)
U ppm							0.17	(d) 0.198	(b)

technique: (a) conventional wet, (b) IDMS, (c) INAA, (d) SSMS, (e) RNAA

**Table 1b. Chemical composition of 12022.**

reference	Baedecker71	Snyder97
<i>weight</i>		
SiO <sub>2</sub> %		43.2
TiO <sub>2</sub>		5.16
Al <sub>2</sub> O <sub>3</sub>		9.04
FeO		21.44
MnO		0.25
MgO		10.43
CaO		9.56
Na <sub>2</sub> O		0.47
K <sub>2</sub> O		0.07
P <sub>2</sub> O <sub>5</sub>		0.13
S %		
<i>sum</i>		
Sc ppm		
V		
Cr		3300
Co		52.6
Ni		47.4
Cu		17.6
Zn	2	(e) 11.5
Ga	3.9	(e) 4.24
Ge ppb		
As		
Se		
Rb		0.841
Sr		142.5
Y		64.2
Zr		160.1
Nb		7.04
Mo		
Ru		
Rh		
Pd ppb		
Ag ppb		105
Cd ppb	6.4	(e)
In ppb	1.6	(e)
Sn ppb		
Sb ppb		
Te ppb		
Cs ppm		
Ba		0.058
La		58.4
Ce		6.5
Pr		17.9
Nd		3.35
Sm		19.2
Eu		6.58
Gd		1.45
Tb		7.94
Dy		1.66
Ho		10.39
Er		2.1
Tm		5.81
Yb		0.82
Lu		5.36
Hf		0.78
Ta		0.78
W ppb		
Re ppb		
Os ppb		
Ir ppb	0.09	(e)
Pt ppb		
Au ppb		
Th ppm		0.987
U ppm		0.28

technique: (e) RANAA, (f) ICP-MS

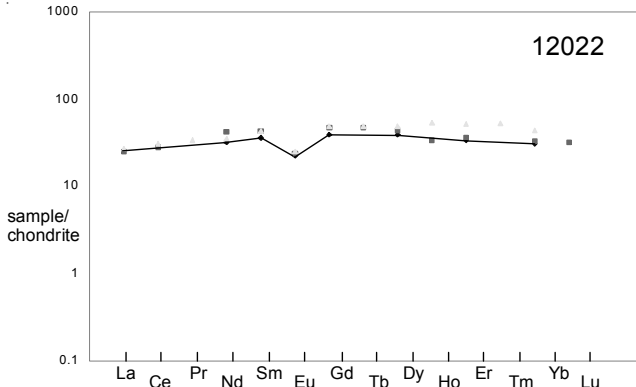


*Figure 6: Comparison of rare-earth-element composition of 12022 by neutron activation analysis (Haskin et al. 1971) and spark-source mass spectroscopy (Taylor et al. 1971) with isotope dilution mass spectroscopy (line, Hubbard and Gast 1971, Wiesman et al. 1975).*

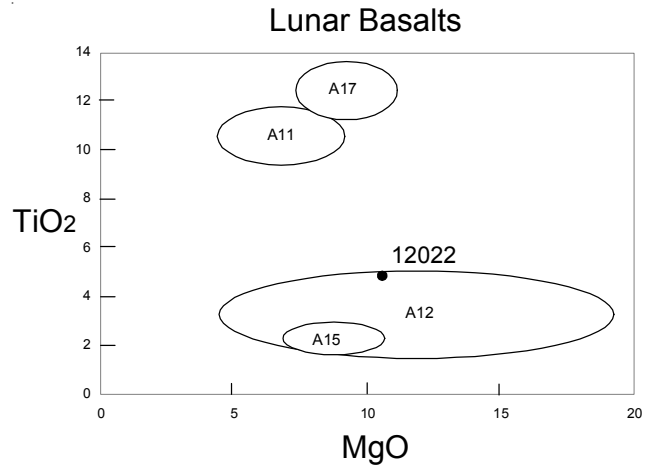


*Figure 7: Composition of 12022 compared with that of other lunar basalts.*

## Other Studies

Bogard et al. (1971) reported the content and isotopic composition of rare gases in 12022. Barber et al. (1971) determined the track density and erosion rate (figure 8).

Helsley (1971) found that 12022 has significant magnetic remanence and Chung et al. (1971) determined the dielectric properties.

Gibson and Hubbard (1972) experimentally studied the volatile depletion for 12022.

## Processing

A thick slab (B,14) was cut from the middle of 12022 with a circular saw (figure 9) and a column (,17) was cut from the slab with a wire saw (figure 12). End piece (A,13) was also subdivided with a wire saw (figure 10). A large piece of 12022 is on public display in Wales, England (figure 13).

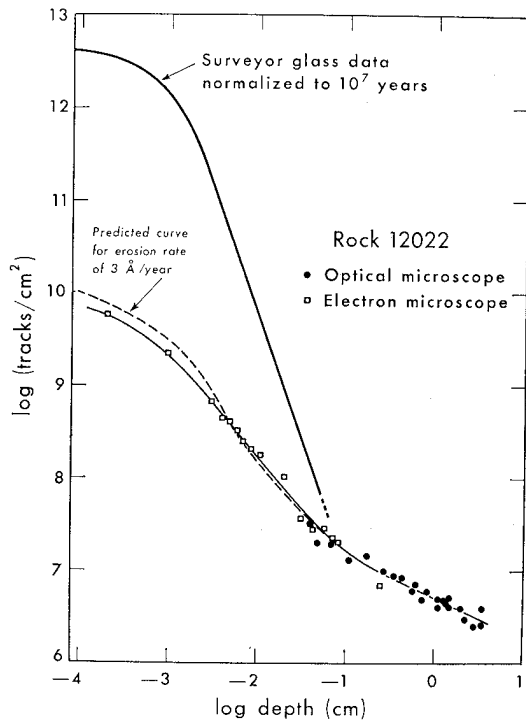


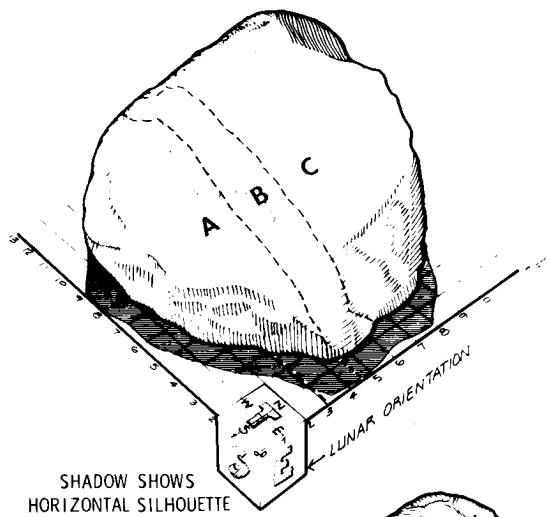
*Figure 8: Track density as function of depth in 12022 (from Barber et al. 1971).*

## List of Photo #s for 12022

S69-64083	color mug
S69-64108	color mug
S70-16784 - 785	TS color
S70-20956	TS color
S70-49560 - 561	
S70-49455 - 460	TS color
S74-24900 - 902	display
S79-27121 - 122	TS color

THE CUTTING OF LUNAR ROCK NO. 12022

DRAWING COMPLETED MAY 13, 1970



THE CUTTING OF SLICE 'A' NO. 12022,13

DRAWING COMPLETED MAY 29, 1970

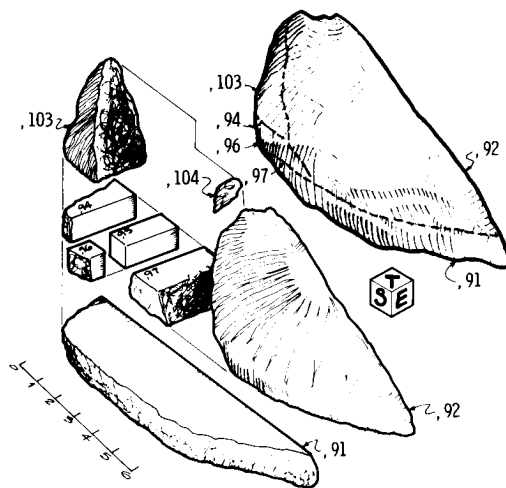
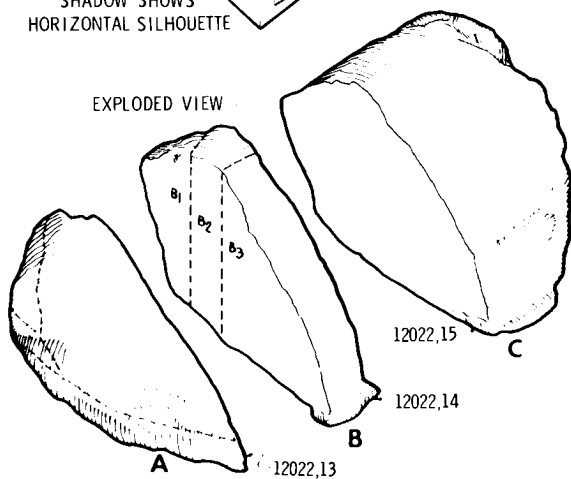
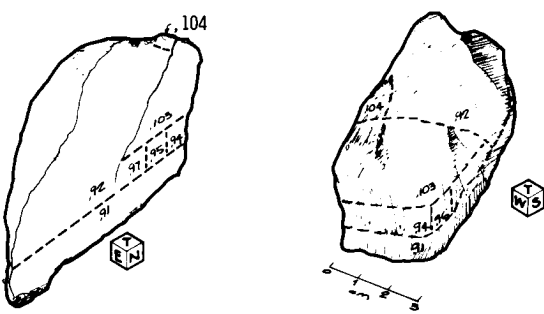


Figure 9: Group photo of 12022,0 after 1.5 mm slab was cut.



Figure 10: Group photo of 12022,13. Scale is in mm.

THE CUTTING AND CHIPPING

OF SLICE 'B' NO. 12022,14

DRAWING COMPLETED MAY 25, 1970

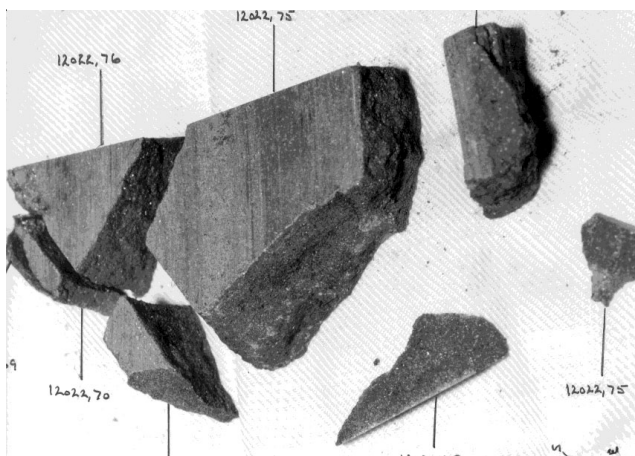
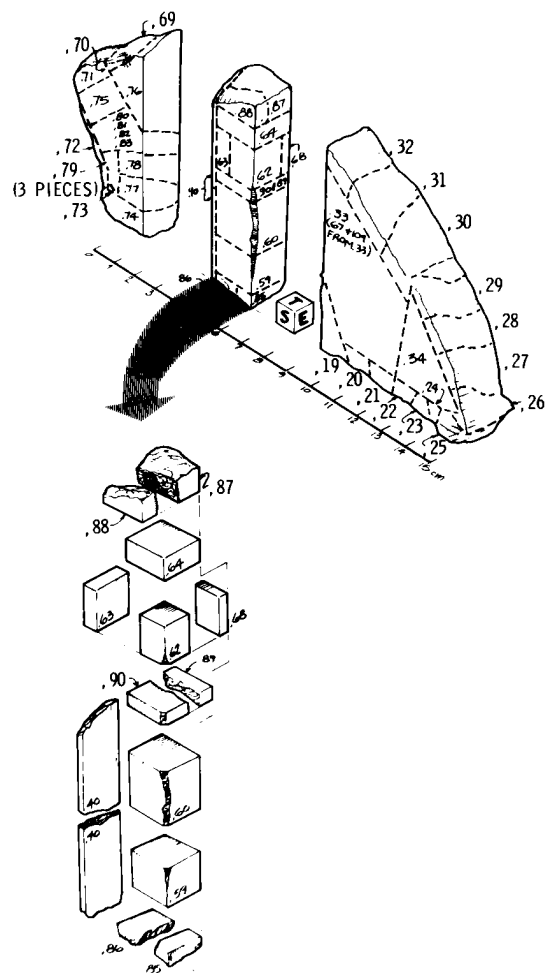


Figure 11: End piece of slab 12022, 14.

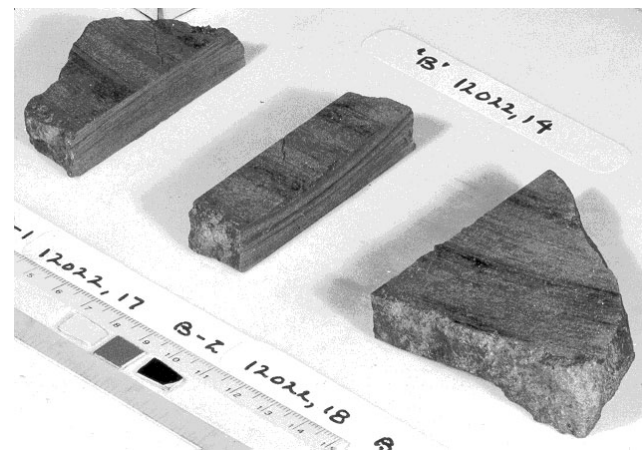
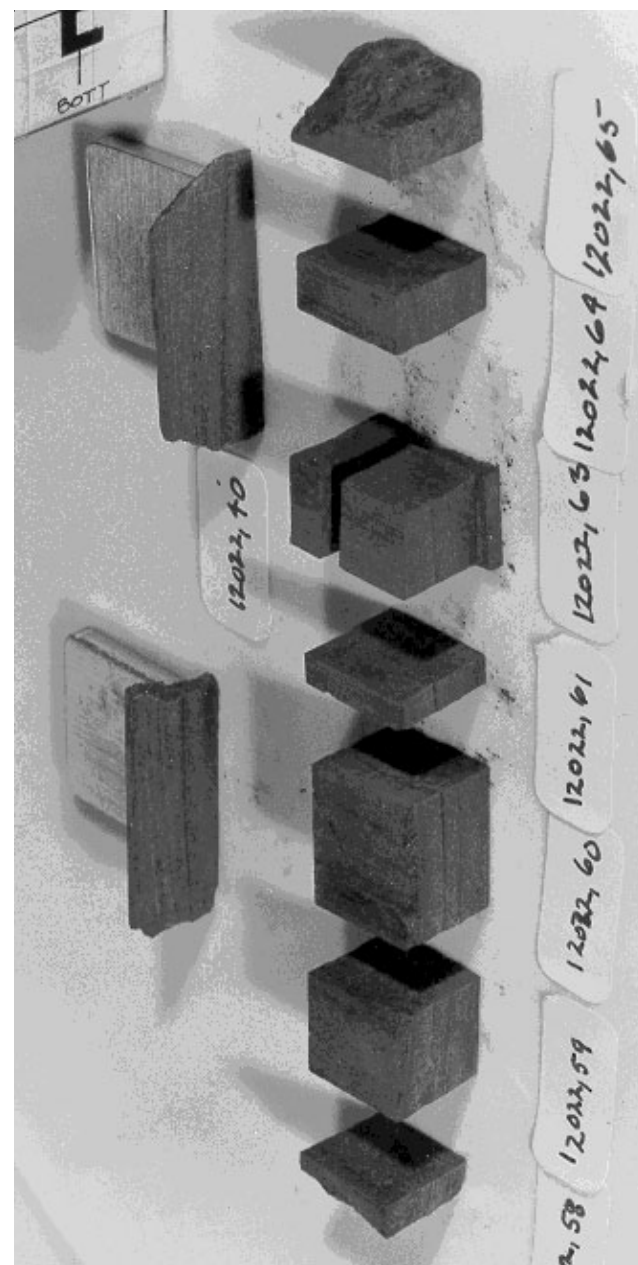
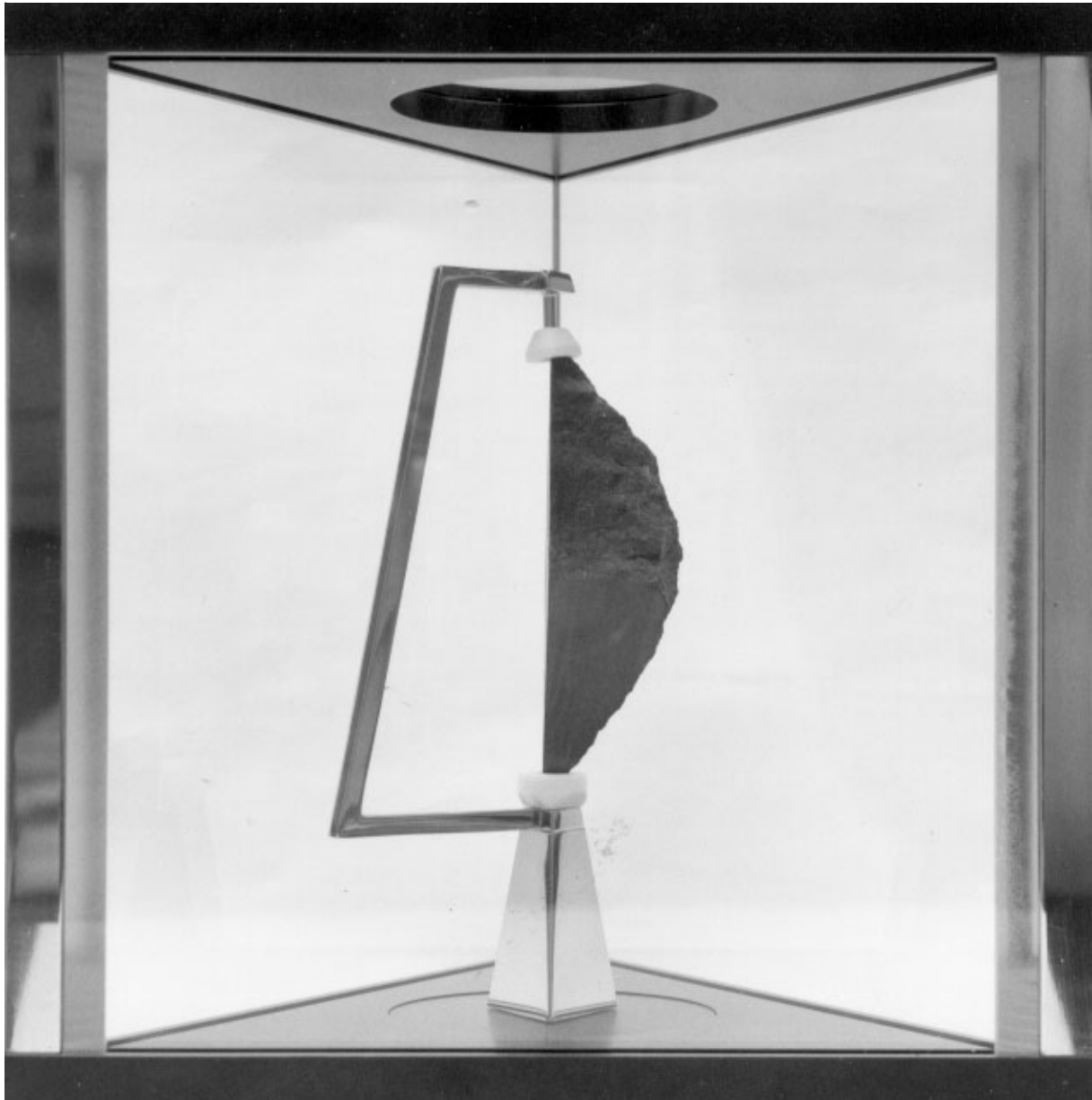


Figure 12: Column (12022,17) cut from slab (12022,14). Scale in mm.





*Figure 13: Display case for 12022,92. NASA S74-24901.*